

On some RF Three-dimensional Simulations of Magnetically Coupled Cells

Marie Chanudet

Laboratoire de l'Accélérateur Linéaire
IN2P3-CNRS et Université Paris-Sud,
Centre d'Orsay, 91405 ORSAY Cedex, France

Abstract

The study of an accelerating structure, without cylindrical symmetry, by means of a 3-D electromagnetic code gives a better knowledge of the electromagnetic properties of the structure. In particular it allows to compute some important RF characteristics for comparison with either analytical method or prototype measurement.

1 INTRODUCTION

In a backward travelling wave structure, the cells are magnetically coupled through some small apertures located out off the axis. Then the cylindrical symmetry is broken and to entirely simulate the electromagnetic field, 3-D computer codes are necessary. The package ANTIGONE (3-D) [1] was used to calculate resonant modes. The present study deals with a particular S band accelerating section operating at $3\pi/4$ mode in which the magnetically coupled cells have different geometries without smooth transition between low field cells and high field cells with longer noses (see figure 1).

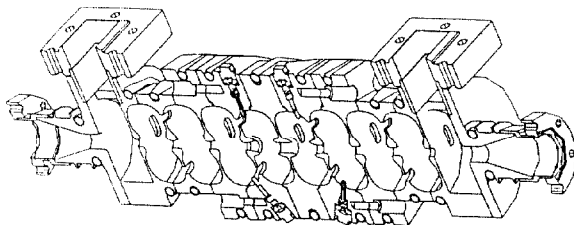


Figure 1: The backward wave section MECCANO

First, the two types of cells are studied separately. When the magnetic coupling holes between the cells are meshed, the program gives directly the frequencies, dispersion curve and coupling coefficient for the fundamental mode as well as for higher order modes. If the coupling aperture is not meshed, an analytical approach also permits to calculate the coupling coefficient [2] and to compare it to the foregoing simulations. Several significant RF characteristics are determined for every cell, for instance three methods to find the effective shunt impedance in the case of a phase advance per cell of $3\pi/4$ are proposed, performed and compared.

2 COUPLING BETWEEN CELLS

For each type of geometry, a three-dimensional mesh composed of tetrahedrons of various dimensions describes two

half volumes joined by the coupling apertures and beam tube. To limit the number of mesh points, only one quarter of the cavity in the azimuthal direction is generated.

2.1 Dispersion Curve

With Neuman boundary conditions, the code ANTIGONE can, of course, calculate the 0 and π modes. Moreover, the phase advance can be forced between identical extremal planes of the cavity. So, one single cavity is sufficient to compute precisely the frequency variations with the phase advance. This program also provides two methods of resolution: the E or B formulation. The wave equation applied to the electric field E (or magnetic field B) is numerically solved in determining the E (or B) flux along the mesh lines. Once E (or B) are calculated, the complementary components B (or E) are deduced from the Maxwell's mixed equations [1]. Two different dispersion curves calculated from E and B formulations are shown in figure 2, where the measured dispersion curve is just sitting in between.

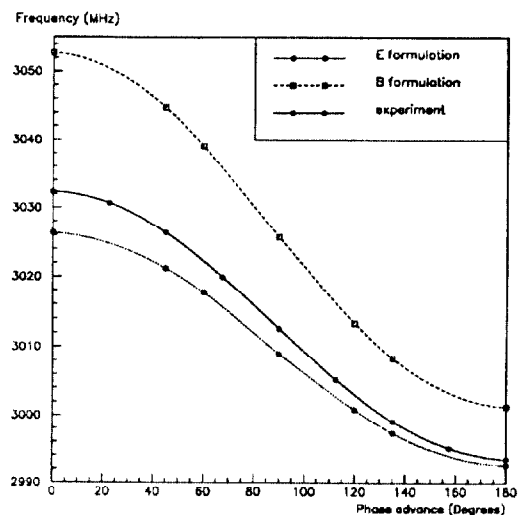


Figure 2: Dispersion curves of the low field cavity

These data also are correctly fitted by the classical formula of dispersion

$$\omega_{\theta}^2 = \omega_{\pi/2}^2 (1 + k \cos \theta) \quad (1)$$

where θ is the phase advance per cell, ω_{θ} is the corresponding angular frequency and k is the coupling coefficient (if $k > 0$ the coupling is mainly magnetic, if $k < 0$ it is electric).

2.2 First Passbands

The first modes of the two types of cells have been simulated and compared to TM_{nml} and TE_{nml} modes of cylindrical cavities. Since the used meshes describe only one quarter of the cell, they are delimited by two perpendicular planes containing the mechanical axis. Each plane is treated by the code as a boundary condition (B.C.) of either metallic or symmetric. This choice implies a fictive polarization of the field in the cell. If the two planes are metallic (mm), the field variations with the azimuthal angle ϕ are $\cos(n\phi)$ or $\sin(n\phi)$ like with n even; then only the TM_{nml} modes with n even are calculated. If the planes are different, and either the metallic one cuts the coupling aperture (ms) or does not (sm), only the TM_{nml} modes with n odd are found. For frequencies less than 7000MHz the results computed with E formulation are shown in table 1.

Table 1: First modes for high and low field cells

Modes	B.C.	High field cell		Low field cell	
		$f_{\pi/2}$ MHz	k $\times 10^{-3}$	$f_{\pi/2}$ MHz	k $\times 10^{-3}$
TM_{010}	ss	2988.93	9.39	3008.98	11.22
TM_{110}	sm	5534.31	5.30	5056.45	11.40
TM_{110}	ms	5547.55	2.06	5085.60	0.24
TM_{210}	ss	7317.36	-1.04	6599.38	3.81
TM_{020}	ss	6808.68	3.93	6781.45	2.47

For the two types of cell, the same TM_{nml} modes appear in the same order as with a perfectly cylindrical cavity, all except the inversion of TM_{020} and TM_{210} modes for the high field cell. The explanation is that the introduction of a metallic nose in an electric field decreases the resonant frequency and the larger are its dimensions and the magnitude of the E field, the stronger is the variation.

2.3 Semi-analytical approach

The coupling coefficient in equation (1) can be also deduced from a perturbative method [2]. Opening an aperture in a cavity creates a shift of the resonant frequency. If the aperture has an elliptical shape of small dimensions compared to the wave length and if the electromagnetic field is uniform on this region, the new frequency can be calculated. In the case of a phase advance per cell equals to θ , the new frequency becomes

$$\begin{aligned} \frac{f^2}{f_0^2} = & 1 + 2N \frac{\pi(1-\epsilon_0^2) l_1^3}{12 E(\epsilon_0)} \frac{\epsilon_0 E_3^2}{U} (1 - \cos\theta e^{-\alpha_3 b}) \\ & - 2N \frac{\pi \epsilon_0^2 l_1^3}{12 [K(\epsilon_0) - E(\epsilon_0)]} \frac{B_1^2}{\mu_0 U} (1 - \cos\theta e^{-\alpha_1 b}) \\ & - 2N \frac{\pi(1-\epsilon_0^2) l_1^3}{12 [E(\epsilon_0) - (1-\epsilon_0^2)K(\epsilon_0)]} \frac{B_2^2}{\mu_0 U} (1 - \cos\theta e^{-\alpha_2 b}) \end{aligned} \quad (2)$$

where f_0 is the resonant frequency of the cavity without aperture, N the number of similar apertures opened in the cavity, b the depth of the coupling aperture, $2l_1$ and $2l_2$ the lengths of the major and minor axes of the elliptical aperture, $\epsilon_0 = (1 - l_2^2/l_1^2)^{1/2}$, $K(\epsilon_0)$ and $E(\epsilon_0)$ the elliptical integrals of the first and second kinds, E_3 , B_1 and

B_2 the fields on the metallic walls at the center of the coupling apertures before they are opened (see figure 3), U the stored energy in the cavity and α_1 , α_2 , α_3 the attenuation coefficients inside the aperture.

The results obtained with E formulation for the high field type of cell when the coupling aperture is not meshed are given in table 2. A reason of the discrepancy of these values with 3-D simulation ones is that the numerical calculations are not very accurate. In the case of high order modes, the difference is larger than for the fundamental because the field varies more rapidly with r and ϕ and the hypothesis that the fields are uniform over the region of the coupling aperture becomes wrong.

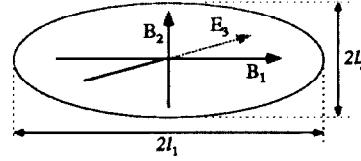


Figure 3: Elliptical aperture and the E_3 , B_1 , B_2 fields

Table 2: Analytical method for high field cell

Modes	B.C.	E_3, B_1, B_2 av.		E_3, B_1, B_2 max.	
		$f_{\pi/2}$ MHz	k $\times 10^{-3}$	$f_{\pi/2}$ MHz	k $\times 10^{-3}$
TM_{010}	ss	2976.44	8.45	2974.54	9.58
TM_{110}	sm	5562.52	0.88	5558.79	3.51
TM_{110}	ms	5547.51	1.39	5542.22	1.48
TM_{020}	ss	6831.51	0.61	6813.28	4.77
TM_{210}	ss	7319.29	-1.18	7321.28	-1.16

3 SHUNT IMPEDANCE

If the 3-D code well simulates the magnetic coupling, the knowledge of the electromagnetic field, the energy stored in the cavity and the losses in the walls will allow to determine the magnitude of the effective shunt impedance. It is usually expressed as:

$$r = \frac{(\int_0^l e_z dz)^2}{P_{o-l}} \quad (3)$$

where r is the effective shunt impedance per unit length, l is the section length, e_z is the electric field seen by the particle and P_{o-l} is the power lost along the distance l . Since the structure operates in a travelling wave with a phase advance of $3\pi/4$ per cell and since the program computes standing waves, three methods to calculate the effective shunt impedance of the $3\pi/4$ mode are proposed, with the aim of limiting the number of mesh points.

3.1 From $3\pi/4$ mode with two cells

The phase advance per cell being equal to $3\pi/4$, it becomes $3\pi/2$ for two cells and the $3\pi/4$ mode can be obtained by generating a mesh with only two cells and setting the boundary conditions either symmetric or metallic at the

end planes. Using the properties of the waves in a periodic structure for $\theta = 3\pi/4$ and the previous boundary conditions, the equation (3) after a simple calculation becomes

$$r^{tw} = 2 \frac{(E_{z0}/2)^2 2d}{P_{0-2d}^{sw}} \quad (4)$$

where tw indicates the travelling wave and sw the standing one, E_{z0} is the fundamental amplitude of the stationary wave, d the length of one cell and P_{0-2d}^{sw} the wall losses for the two cells.

3.2 From $3\pi/4$ mode with one cell

Another method using the possibility to set the $3\pi/4$ phase advance between two identical planes of a single cell and the expansion in space harmonics of the magnetic field has also been performed [3]. Corresponding results are shown in table 3.

3.3 From π mode

As the diameter of the iris of the cells is small (<7 .mm), the electric field on the axis is very small at the location of the iris. In the first half volume the electric field pattern E_z^π of the π mode is similar to that of the $3\pi/4$ mode. The electric field E_z of the $3\pi/4$ mode is then reconstituted along the two cells with the relations:

$$\begin{aligned} E_z(z) &= E_z^\pi(z) && \text{if } 0 < z < d/2, \\ E_z(z) &= \cos(3\pi/4) * E_z^\pi(d-z) && \text{if } d/2 < z < d, \\ E_z(z) &= \cos(3\pi/4) * E_z^\pi(z-d) && \text{if } d < z < 3d/2, \\ E_z(z) &= 0 && \text{if } 3d/2 < z < 2d. \end{aligned}$$

Assuming the losses are proportional to the square of E_z , they are approximated for $3\pi/4$ mode by $P_{0-2d} \simeq 2 P_{0-d/2}^{sw}$. Finally, the shunt impedance becomes equal to

$$r^{tw} \simeq 2 \frac{(E_{z0}/2)^2 2d}{2P_{0-d/2}^{sw}} \quad (5)$$

3.4 Validity

The calculated shunt impedances are presented in table 3. The three methods are validated by the fact that the maximum difference of 7% between the different results is less than the estimated measurement error of 10%. They should be generalized to other values of phase advance. The method using two cells appears as the most natural and is surely the most accurate because it uses a formula without approximation. Moreover, the π mode is very simple and gives a good performance although rough approximation is used.

Table 3: Shunt impedance for the high field cell

form.	method		E_{z0} MV/m	P_{0-2d} W	r^{tw} M Ω /m
	mode	nb cell			
E	$3\pi/4$	2	0.547	25.90	108.52
	π	1	0.546	26.05	107.39
B	$3\pi/4$	2	0.596	29.07	114.6
	$3\pi/4$	1	0.597	29.11	114.98
	π	1	0.597	29.63	112.7

4 OTHER RF CHARACTERISTICS

A more complete analysis of the simulations gives additional RF characteristics for the accelerating structure such as the quality factor Q , the group velocity v_g or the attenuation coefficient α . The simulated and measured values appear to be in very good agreement as shown in table 4.

The visualization of the electromagnetic field in all the meshed volume allows the study of the problem as a whole. So, the variations of the field may be observed (particularly the points of maximum electric amplitude on the metallic surface.)

Table 4: RF characteristics for the low field cell

	$f_{3\pi/4}$ MHz	k $\times 10^{-3}$	Q	c/v_g	r^{tw} M Ω /m	α Nep.
Sim.	2997.02	11.2	1300	104	95	0.12
Exp.	2998.07	12.7	-	94	93	0.11

5 CONCLUSION

The computer simulations of a magnetically coupled structure made of different cell geometries (low field and high field volumes) have shown that the 3-D code ANTIGONE is quite well suited due to its ability of setting the phase advance per cell and because it offers the two types of field formulations (E and B). Consequently the difficulties of a 3-D meshing for long structures together with the time consumption are partly overcome.

6 ACKNOWLEDGEMENTS

I would like to thanks G. Bienvenue, P. Brunet, J. Gao, J. Le Duff, G. Le Meur and F. Touze for constant help or support.

7 REFERENCES

- [1] G. Le Meur and F. Touze, "PRIAM/ANTIGONE: A 2D/3D Package For Accelerator Design", these proceedings.
- [2] J. Gao, "Analytical formulas for the resonant frequency changes due to opening apertures on cavity walls", Nucl. Instr. and Meth., A311(1992) 437-443.
- [3] M. Chanudet, "Simulations 3-D de la Cavité Fort Champ de la Section MECCANO", (Internal Note LAL, SERA 93-519, Sept. 1993)